

TAK1 regulates skeletal muscle mass and mitochondrial function

By

**Sajedah M. Hindi, Shuichi Sato, Guangyan Xiong, Kyle R. Bohnert, Andrew A. Gibb,
Yann S. Gallot, Joseph D. McMillan, Bradford G. Hill, Shizuka Uchida, and Ashok Kumar**

This file contains:

- 1). Figure S1-S7 and their Legends
- 2). Table S1, S2

FIGURE S1

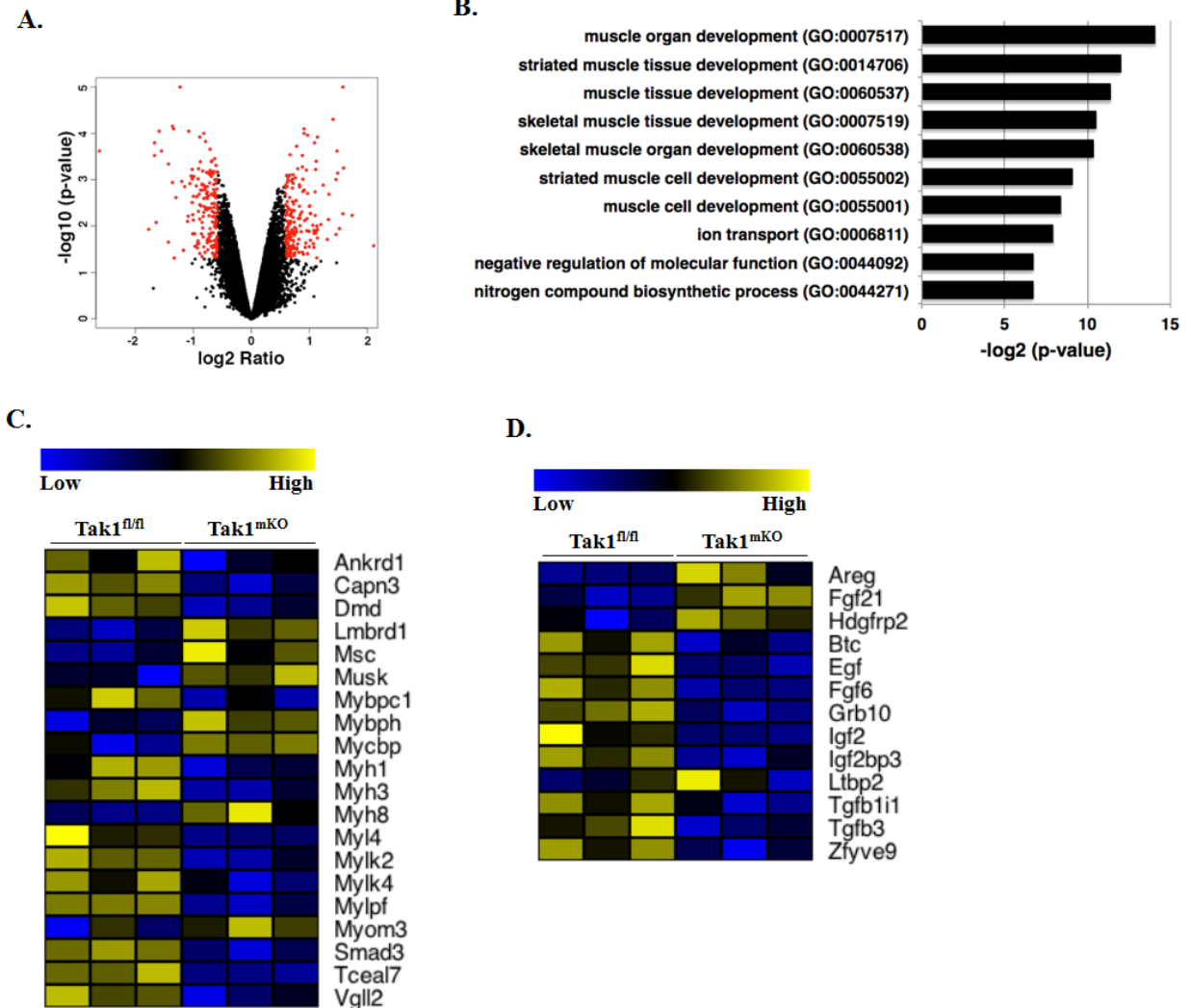


Figure S1. Microarray analysis of gene expression in skeletal muscle of $Tak1^{fl/fl}$ and $Tak1^{mKO}$ mice. (A) Volcano plot of expression changes. The differentially expressed genes (1.5-fold; $p < 0.05$) are shown in red. (B) Gene ontology (GO) analysis of differentially expressed genes. Top 10 GO terms enriched under the biological processes are shown. Heat map of some of (C) skeletal muscle genes, and (D) growth factors differentially regulated in skeletal muscle of $Tak1^{fl/fl}$ and $Tak1^{mKO}$ mice. The genes upregulated in the microarray data are shown in red, while those of downregulated ones are shown in green. $n=3$ in each group.

FIGURE S2

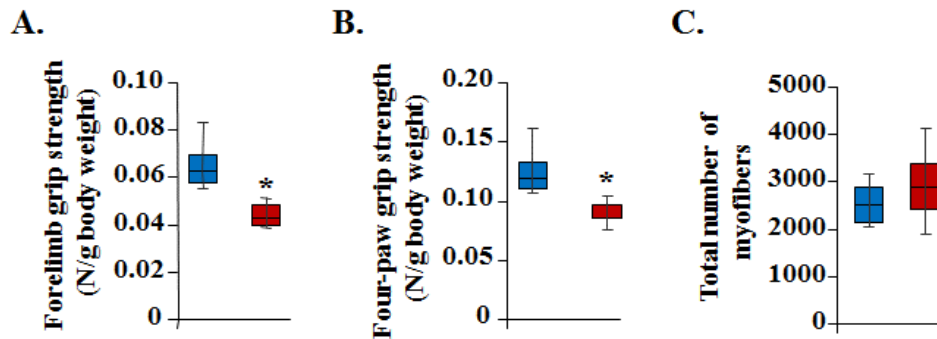


Figure S2. Ablation of TAK1 reduces grip strength in adult mice. 14-week-old Tak1^{fl/fl} and Tak1^{mKO} mice were treated with tamoxifen and 10 weeks later their grip strength was measured. **(A)** Average forelimb and **(B)** average four-paw grip strength in Tak1^{fl/fl} and Tak1^{mKO} mice normalized with their body weight. **(C)** Average number of myofibers in TA muscle sections of Tak1^{fl/fl} and Tak1^{mKO} mice. n=6 in each group. Error bars represent \pm SEM. *p<0.05 values significantly different from corresponding Tak1^{fl/fl} mice by unpaired two-tailed t-test.

FIGURE S3

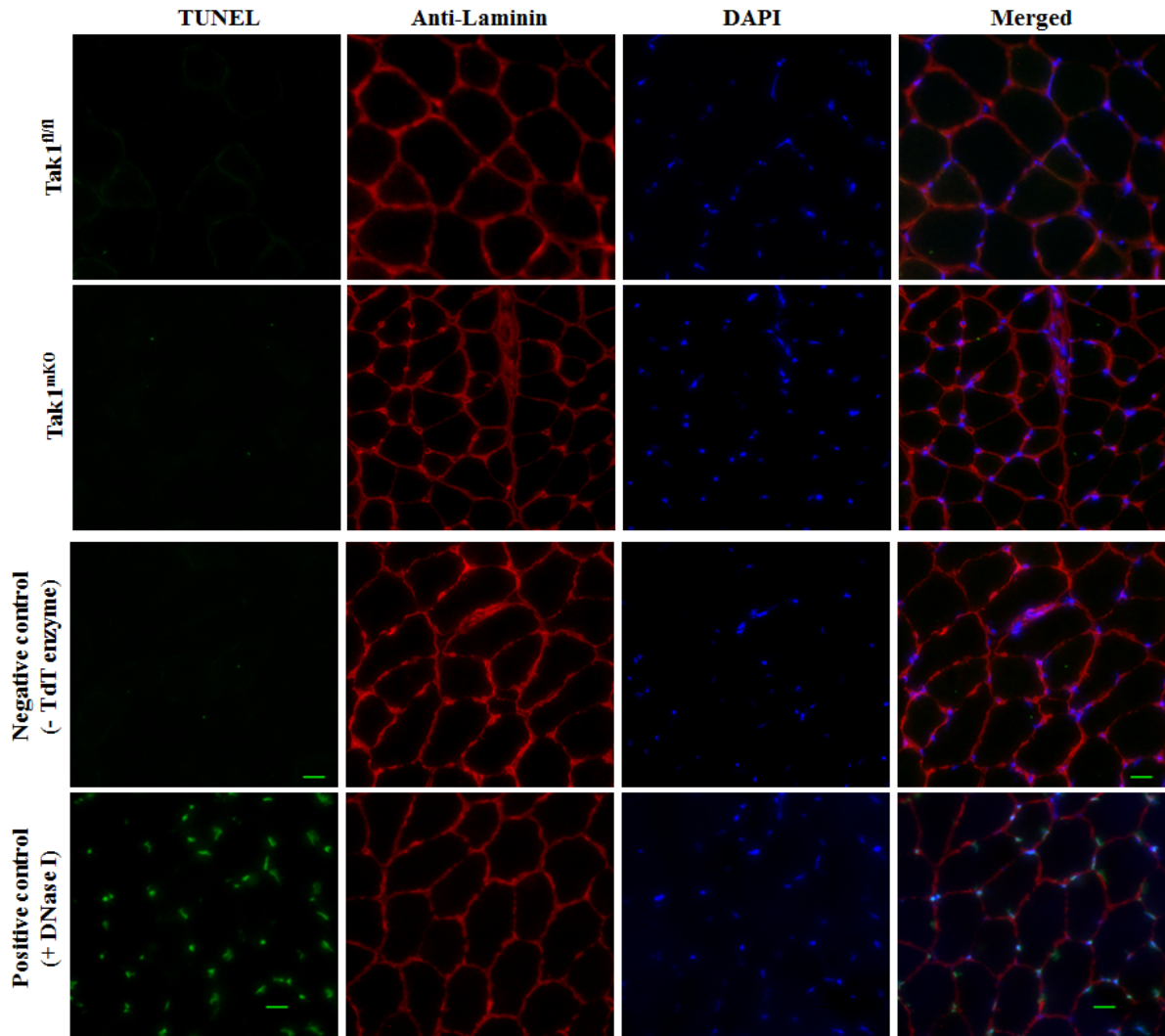


Figure S3. Ablation of TAK1 does not induce apoptosis in skeletal muscle. 14-week-old Tak1^{fl/fl} and Tak1^{mKO} mice were treated with tamoxifen and 10 weeks later, the mice were euthanized and TA muscle was collected and processed for TUNEL staining. The sections were also stained for laminin. Nuclei were counterstained with DAPI. Representative merged images are presented here (upper two panels). Lower two panels represent negative and positive (i.e. DNase I treated) muscle sections. Scale bars: 20 μ m.

FIGURE S4

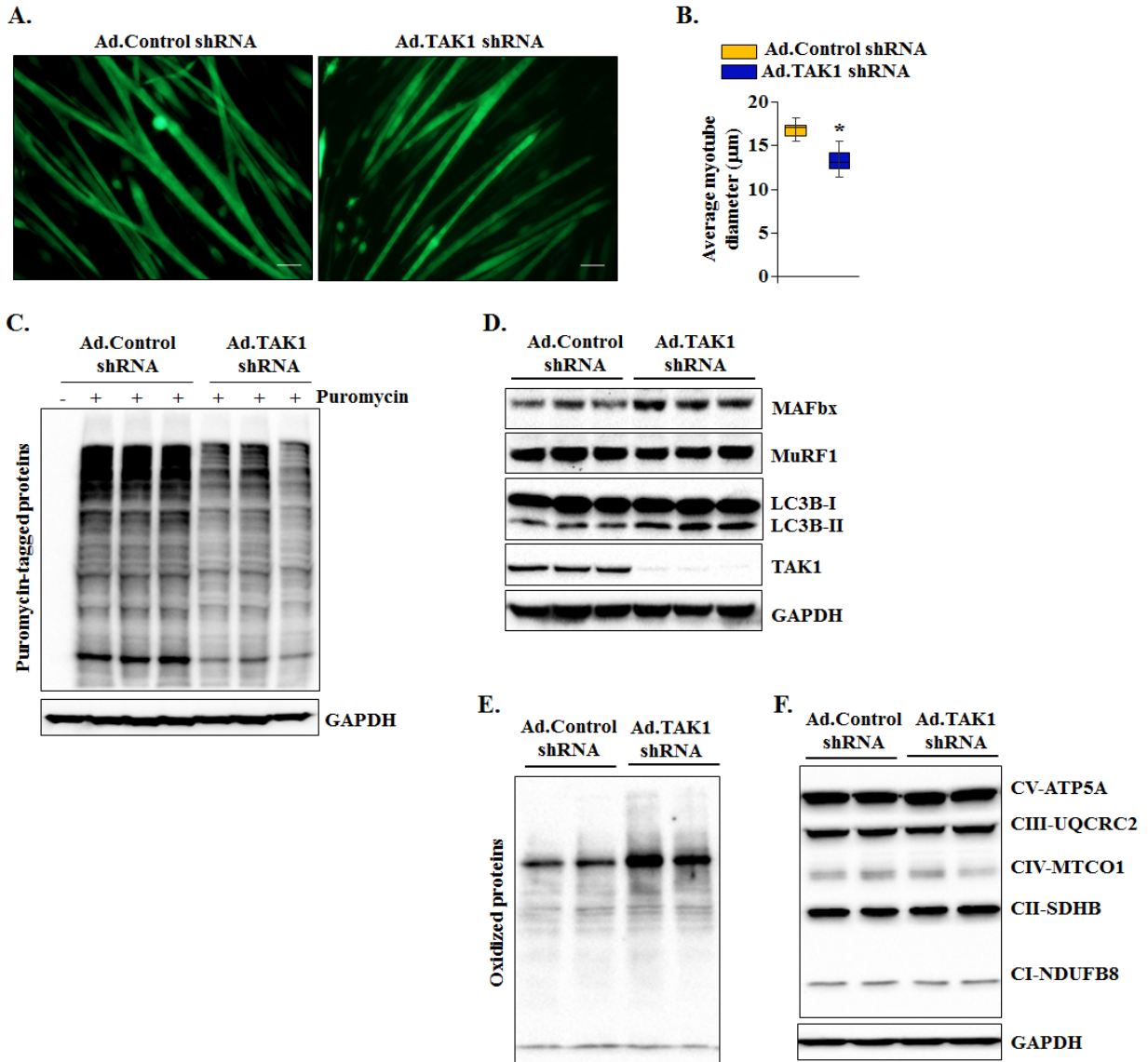


Figure S4. Effects of knockdown of TAK1 in culture myotubes. Primary myoblasts prepared from hind limb muscle of WT mice were differentiated into myotubes, followed by addition of Ad.Control shRNA or Ad.TAK1 shRNA at MOI 1:50. After 48h, the cultures were fixed and examined under a fluorescence microscope. **(A)** Representative photomicrographs of myotube cultures. Scale bars: 50 μm . **(B)** Quantification of the average diameter of myotubes in control shRNA- and TAK1 shRNA-expressing cultures. $n=10$ in each group. Error bars represent \pm SEM. $*p<0.05$ values significantly different from corresponding Ad.TAK1 shRNA cultures by unpaired two-tailed t-test. **(C)** In a separate experiment, myotubes were transduced with Ad.Control shRNA or with Ad.TAK1 shRNA for 48h. The myotubes were treated with 1 μM

puromycin for exactly 30 min followed by analysis for puromycin-tagged proteins.

Representative immunoblot demonstrating the levels of puromycin-tagged protein in Ad.Control shRNA and Ad.TAK1 shRNA cultures. **(D)** Protein levels of MAFbx, and MuRF1, LC3B-I/II, and TAK1 in control shRNA- and TAK1 shRNA-expressing myotube cultures. **(E)**

Representative immunoblot demonstrating the levels of carbonylated protein in Ad.TAK1 shRNA and Ad.Control shRNA myotube cultures. **(F)** Immunoblot demonstrating the protein levels of the 5 OXPHOS complexes in Ad.TAK1 shRNA and Ad.Control shRNA myotube cultures. N=3-5 in each group. Error bars represent \pm SEM. * $p < 0.05$, values significantly different from corresponding Ad.Control shRNA cultures by unpaired two-tailed t-test.

FIGURE S5

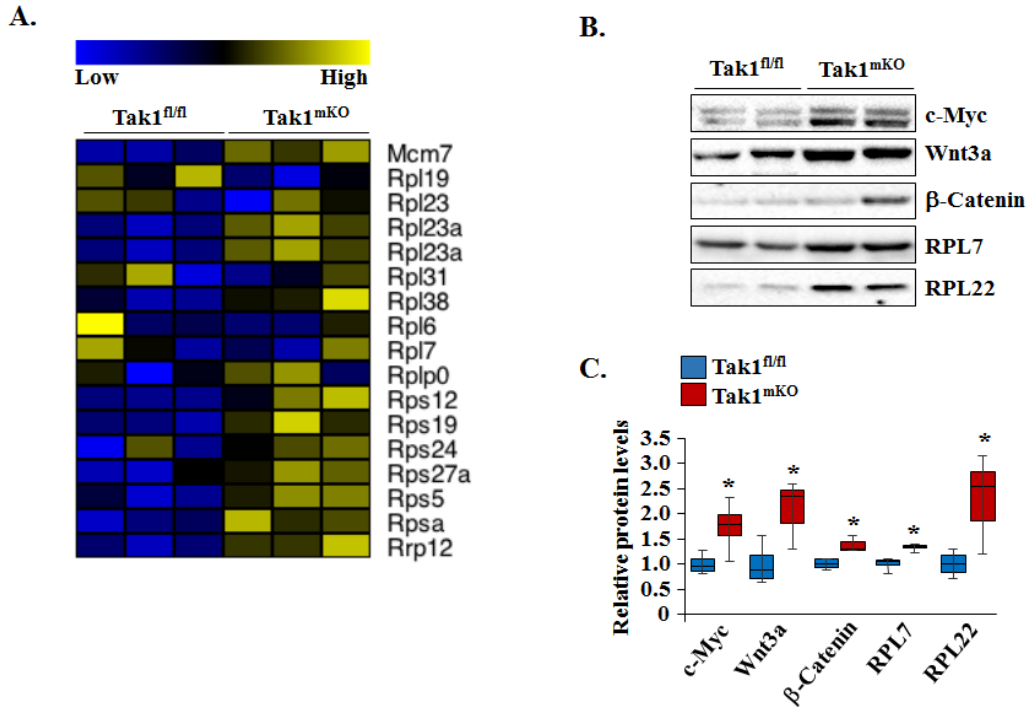
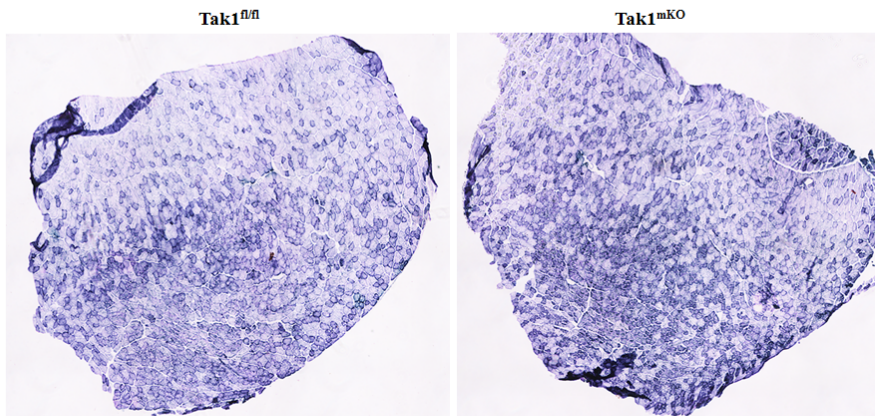


Figure S5. Role of TAK1 in ribosomal biogenesis in skeletal muscle of mice. (A) Heat map showing gene expression of various ribosomal protein in skeletal muscle of *Tak1^{fl/fl}* and *Tak1^{mKO}* mice evaluated by microarray analysis. N=3 in each group. (B) Protein levels of c-Myc, Wnt3a, β -catenin, RPL7, and RPL22 in skeletal muscle of *Tak1^{fl/fl}* and *Tak1^{mKO}* mice measured by Western blot. (C) Densitometry analysis of levels of c-Myc, Wnt3a, β -catenin, RPL7, and RPL22 in skeletal muscle of *Tak1^{fl/fl}* and *Tak1^{mKO}* mice. N=4 or 5 in each group. Error bars represent \pm SEM. * $p < 0.05$, values significantly different from corresponding *Tak1^{fl/fl}* mice by unpaired two-tailed t-test.

FIGURE S6

A.



B.

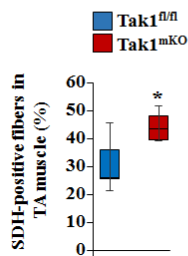


Figure S6. Succinate dehydrogenase (SDH) staining analysis for oxidative capacity. (A) TA muscle sections from $Tak1^{fl/fl}$ and $Tak1^{mKO}$ mice were stained for SDH. Representative photomicrographs of SDH-stained muscle sections are presented here. **(B)** Quantification of the percentage of SDH-positive fibers in skeletal muscle of $Tak1^{fl/fl}$ and $Tak1^{mKO}$ mice. N= 5 in each group. Error bars represent \pm SEM. * $p < 0.05$, values significantly different from corresponding $Tak1^{fl/fl}$ mice by unpaired two-tailed t-test.

FIGURE S7

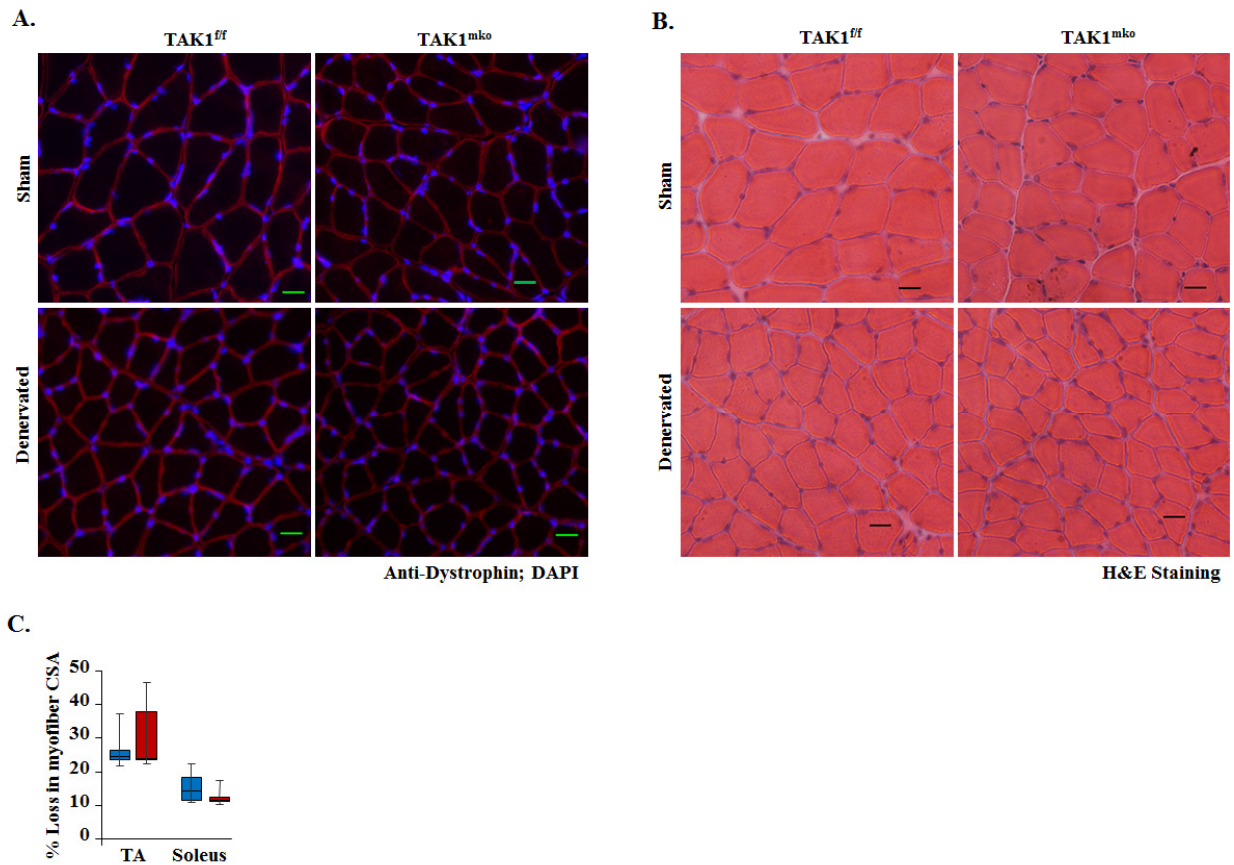


Figure S7. Role of TAK1 in denervation-induced atrophy. Representative photomicrographs of soleus muscle sections of Tak1^{fl/fl} and Tak1^{mKO} mice after (A) anti-dystrophin staining, and (B) H&E-staining. Scale bars: 20 μ m. (C) Percentage loss in myofiber CSA in TA and soleus muscle of Tak1^{fl/fl} and Tak1^{mKO} mice. N = 4 or 5 in each group. Error bars represent \pm SEM. No statistical significant differences was noticed in percentage loss in myofiber CSA between Tak1^{fl/fl} and Tak1^{mKO} mice after denervation by unpaired two-tailed t-test.

Table S1: Antibodies and their dilution used in this study. IHC, immunohistochemistry; IP, immunoprecipitation; WB, Western blot.

Antibody	Source and catalog number	Dilution	Analysis
Polyclonal rabbit-anti-Laminin	Sigma, L9393	1:500	IHC
Polyclonal rabbit-anti-Dystrophin	Abcam, ab15277	1:400;1:500	IHC;WB
Monoclonal mouse-anti-MyHC	DSHB, MF20	1:200;1:1000	IHC;WB
Polyclonal rabbit-anti-TAK1	Cell Signaling Technology, # 4505	1:500	WB
Polyclonal rabbit anti-TAB1	Cell Signaling Technology, # 3225	1:500	WB
Polyclonal rabbit-anti-TRAF6	Santa Cruz Biotechnology, sc-7221	1:500	WB
Monoclonal rabbit-anti-GAPDH	Cell Signaling Technology # 2118	1:2000	WB
Monoclonal mouse-anti-Tropomyosin	Sigma, T9283	1:500	WB
Monoclonal mouse-anti-Troponin	Sigma, T6277	1:500	WB
Monoclonal mouse-anti-Sarcomeric α -actin	Sigma, A2172	1:500	WB
Monoclonal mouse-anti-Puromycin	Millipore, MABE343	1:1000	WB
Monoclonal mouse-anti-Ubiquitin	Santa Cruz Biotechnology, sc-8017	1:500	WB
Monoclonal rabbit-anti-phospho-AMPK α	Cell Signaling Technology, # 2535	1:500	WB
Polyclonal rabbit-anti-total AMPK α	Cell Signaling Technology, # 2532	1:500	WB
Monoclonal rabbit-anti-phospho-Akt	Cell Signaling Technology, # 4060	1:500	WB
Polyclonal rabbit-anti-total-Akt	Cell Signaling Technology, # 9272	1:500	WB
Polyclonal rabbit-anti-phospho-mTOR	Cell Signaling Technology, # 2971	1:500	WB
Polyclonal rabbit-anti-total-mTOR	Cell Signaling Technology, # 2972	1:500	WB
Polyclonal rabbit anti-phospho-p38 MAPK	Cell Signaling Technology, # 9211	1:500	WB
Polyclonal rabbit anti-total-p38 MAPK	Cell Signaling Technology, # 9212	1:500	WB
Monoclonal rabbit-anti-phospho-I κ B α	Cell Signaling Technology, # 2859	1:500	WB
Monoclonal rabbit-anti-total I κ B α	Cell Signaling Technology, # 4812	1:500	WB
Polyclonal rabbit-anti-p100/p52	Cell Signaling Technology, # 4882	1:500	WB
Monoclonal rabbit-anti-Total-OXPHOS cocktail	Abcam, ab110413	1:1000	WB
Polyclonal rabbit-anti-PGC-1 α	Santa Cruz Biotechnology, sc-13067	1:500	WB
Monoclonal rabbit-anti-Mitofusin-2	Cell Signaling Technology, # 9482	1:500	WB
Monoclonal rabbit-anti-DRP1	Cell Signaling Technology, # 5391	1:500	WB
Polyclonal rabbit-anti-PINK1	Abcam, ab23707	1:500	WB
Monoclonal rabbit-anti-Beclin-1	Cell Signaling Technology, # 3495	1:500	WB
Polyclonal rabbit-anti-p62 (SQSTM1)	MBL, PM045	1:500	WB
Monoclonal rabbit-anti-phospho-TAK1	Thermo Fisher Scientific, MA5-15073	1:250	WB
Polyclonal rabbit-anti-MAFbx (Atrogin-1)	ECM Biosciences, AP2041	1:500	WB
Polyclonal goat-anti-MuRF1	R&D Systems, AF5366	1:500	WB
Polyclonal rabbit-anti-phospho-4E-BP1	Cell Signaling Technology, # 9455	1:500	WB
Polyclonal rabbit-anti-total-4E-BP1	Cell Signaling Technology, # 9452	1:500	WB
Polyclonal rabbit-anti-c-Myc	Cell Signaling Technology, # 9402	1:500	WB
Polyclonal rabbit-anti-Wnt3a	Millipore, ABD124	1:500	WB
Monoclonal rabbit-anti-active β -Catenin	Cell Signaling Technology, # 19807	1:500	WB
Polyclonal rabbit-anti-RPL7	Novus Biologicals, NB100-2269	1:500	WB
Monoclonal mouse-anti-RPL22	Santa Cruz Biotechnology, sc-136413	1:500	WB
Monoclonal rabbit-anti-TAK1	Cell Signaling Technology, # 5206	1:166	IP

Table S2. Sequence of the primers used for QRT-PCR analyses.

Gene name	Forward primer (5'-3')	Reverse primer (5'-3')
Myh4	CGGCAATGAGTACGTACCAAAA	TCAAAGCCAGCGATGTCCAA
MAFbx/Atrogin-1	GTCGCAGCCAAGAAGAGAAAGA	TGCTATCAGCTCCAACAGCCTT
MuRF1	TACTGCATCTCCATGCTGGTG	TGGCGTAGAGGGTGTCAAACCTT
Nedd4	GTGGGAAGAGAGGCAGGATGTC	GCGAATTCACAGGAAGTGTAGGC
MUSA1	TCGTGGAATGGTAATCTTGC	CCTCCCGTTTCTCTATCACG
LC3B	CTGGTGAATGGGCACAGCATG	CGTCCGCTGGTAACATCCCTT
Beclin-1	TGAAATCAATGCTGCCTGGG	CCAGAACAGTATAACGGCAACTCC
Atg5	ATCAGACCACGACGGAGCGG	GGCGACTGCGGAAGGACAGA
Gabarapl1	CGGTCATCGTGGAGAAGGCT	CCAGAACAGTATAACGGCAACTCC
Atg12	ACAAAGAAATGGGCTGTGGAGC	GCAGTAATGCAGGACCAGTTTACC
CAT	CGGCACATGAATGGCTATGGATC	AAGCCTTCCTGCCTCTCCAACA
GPx1	GGGCTCCCTGCGGGGCAAGGT	ATGTACTTGGGGTCGGTCATG
XDH	ATCTGGAGACCCACTGCACC	TGTGCTCACGAAGAGCTCCAT
Cu/ZnSOD	TGAACCAGTTGTGTTGTCAG	TCCATCACTGGTCACTAGCC
EcSOD	AGGTGGATGCTGCCGAGAT	TCCAGACTGAAATAGGCCTCAAG
MnSOD	TGGCTTGGCTTCAATAAGGA	AAGGTAGTAAGCGTGCTCCCACAC
β -actin	CAGGCATTGCTGACAGGATG	TGCTGATCCACATCTGCTGG